

Effect of different obstacle geometries on deflagration explosion in a vented chamber

Hee Kwon Byun^{*}, Dong Joon Kim^{**}, and Dal Jae Park^{***†}

^{*}Department of Safety Engineering, Graduate School of Industry, Seoul National University of Science & Technology, 232 Gongneung-ro, Nowon-gu, Seoul 01811, KOREA

^{**}Department of Fire Safety Engineering, Kyungil University, 50 Gamasilgil, Hyangup, Gyeongsan, Gyeongbuk 712-701, KOREA

^{***}Department of Safety Engineering, Seoul National University of Science & Technology, 232 Gongneung-ro, Nowon-gu, Seoul 01811, KOREA
Phone: + 82-2-970-6308

[†]Corresponding author: pdj70@seoultech.ac.kr

Received: July 18, 2017 Accepted: April 5, 2018

Abstract

Experimental studies were performed to investigate explosion characteristics involving different obstacle geometries and quantities in a vented explosion chamber. Three different obstacle geometries were explored: square, triangular and cylindrical. The quantity of each type of obstacle within the chamber was increased from one to five. It was found that as the number of obstacles increased, the flame speeds and overpressures increased. It was also found that the triangular obstacle resulted in the highest overpressures and flame speeds, while the lowest was obtained with the circular type. For multiple obstacles, the peak overpressure was highly dependent on the obstacle type. This may be due to the presence of surface edges on the obstacle types used. It is considered that during flame interaction with the obstacles, the sharp edge creates turbulence, resulting in flame accelerated and rising pressure.

Keywords: obstacle geometries, obstacle numbers, flame speed, pressure

1. Introduction

Gas explosion accidents are highly concerning to process industries due to the potential for domino effects and serious consequences¹⁾. Numerous studies have focused on the correlation between the severity of the gas explosion and flame speed²⁾⁻⁴⁾. Furthermore, it is well known that the severity of such explosions is mainly dependent on obstacle density levels^{5), 6)}. The prediction of overpressures resulting from interactions with obstacles has also been of great interest to make sure safer design of installations⁶⁾.

For such predictions, computational fluid dynamics (CFD) are being used in explosion assessments^{7), 8)}. However, available CFD tools have been tested against limited experimental data and should be verified against sufficient experimental data to confirm their reliability as a predictive tool^{8), 9)}. Therefore, additional experimental data

are required to develop turbulent combustion models of CFD.

Over the last twenty years, many researchers¹⁰⁾⁻¹⁵⁾ have investigated the explosion characteristics between a propagating flame and obstacles within chambers that have a large length to diameter ratio (L/D). It has been found that flame speed and peak pressure are sensitive to the size and shape of obstacles. Masri et al.¹³⁾ reported that a square obstacle caused faster flame acceleration than circular and triangular obstacles¹⁶⁾. The trend for flame velocities obtained by Masri et al.¹³⁾ was different from that reported in the literature¹⁷⁾. This reason seems to be associated with the obstructions of different obstacle types used.

Little attention has been paid to examine the explosion characteristics by increasing the number of obstacles for different obstacle geometries in a vented explosion

chamber. The main objectives of this study were to investigate flame and pressure variations by increasing the quantity of different obstacle geometries and to investigate a consistency with those previously reported¹⁷.

2. Experimental

Figure 1 shows a schematic diagram of the experimental setup. The explosion chamber dimensions were 1000 mm in length with 130 × 100 mm² cross-section. The chamber rig was composed of 10 mm thick transparent polycarbonate to allow high-speed flame visualization. Before entering the chamber, the flammable gas (99 % C₂H₆O by volume) was premixed with air using mass flow controllers (Tylan FC-280S) to provide a stoichiometric mix, $\phi = 1$. The flammable mixture was ignited with an ignition energy of approximately 0.56 mJ. The equipment used in this study was the same as that reported in previous study¹.

Three objects with differing geometries were chosen for this study. The dimensions (in mm) of the triangular, square, and cylindrical obstacles were L130×ES29, L130×S30, and L130×D30, where L: Length, ES: Equal Side, S: Side, and D: Diameter. The quantity of each obstacle within the chamber was increased from one to five. The first obstacle was located 100 mm from the closed end of the chamber and subsequent obstacles were located 200 mm apart. Full configuration details of all obstacles used in this study are provided in Table 1. Each test was repeated at least five times to make sure reproducibility, and the averaged

results are reported.

3. Results and discussion

Figure 2 presents differences in the flame front structure as the number of obstacles for each obstacle types increases. Four flame front structures taken at 5 ms intervals from 20–35 ms at are presented in each case. It was clear that the overall downstream flame propagation speed increased as the number of obstacles increased from one to five. The flame front structure and flame geometry were independent of the number of obstacles, as the flame impinged on the first obstacle. It took approximately 20 ms for the flame to reach the first obstacle, and at approximately 25 ms the flame propagated in the wake of the obstacle as two uniform fronts. After approximately 30 ms, the flame geometries containing one to four obstacles were similar; however, in the five obstacle case, the flame front emerged from the gap between the second blockage and the chamber walls. At approximately 35 ms, the differences between single and multiple obstacles became more pronounced. The single obstacle flame propagated in a laminar fashion toward the chamber exit. As the number of obstacles increased from two to four, the distorted flame front was more developed, with a much greater downstream distance upon interaction with the obstacles. The flame was fully developed within the chamber containing five obstacles.

Figure 3 shows examples of the variations of flame speed and pressure versus time within the chamber containing five obstacles for each shape. The flame speed was obtained by measuring the position of the propagating flame front from the ignition point until the

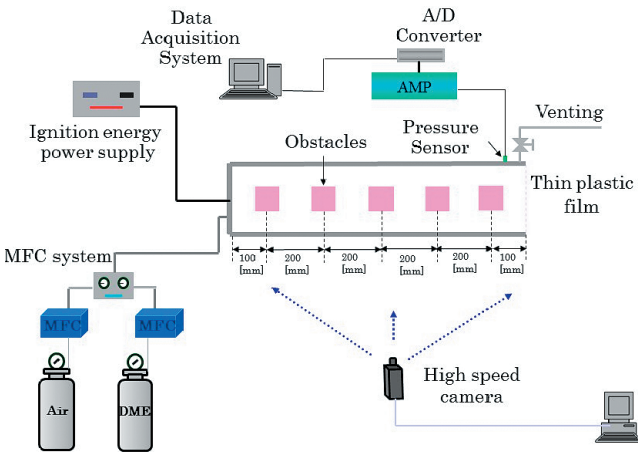


Figure 1 A schematic diagram of the experimental setup.

Table 1 All obstacle configurations used in the tests.

Triangle	Variables			Number of obstacle	D*
	Square	Circle			
T1	S1	C1	1	100	
T2	S2	C2	2	300	
T3	S3	C3	3	500	
T4	S4	C4	4	700	
T5	S5	C5	5	900	

D*: Distance from the closed end of chamber to the middle point of the obstacle

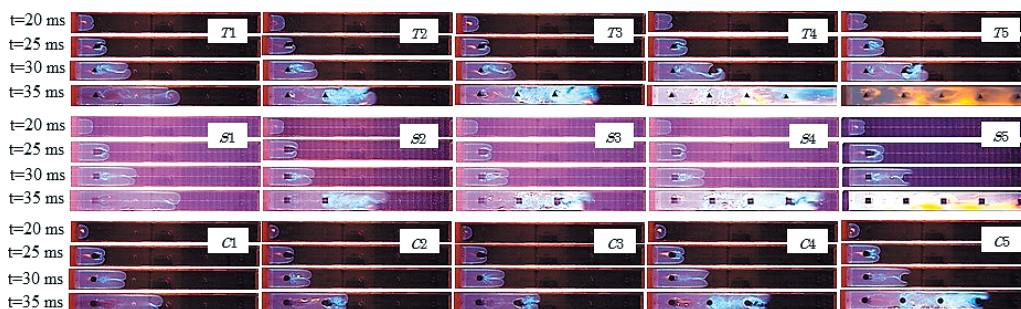


Figure 2 A comparison of representative sequences taken from the flame propagation images for different kinds of obstacles and various obstacles quantities.

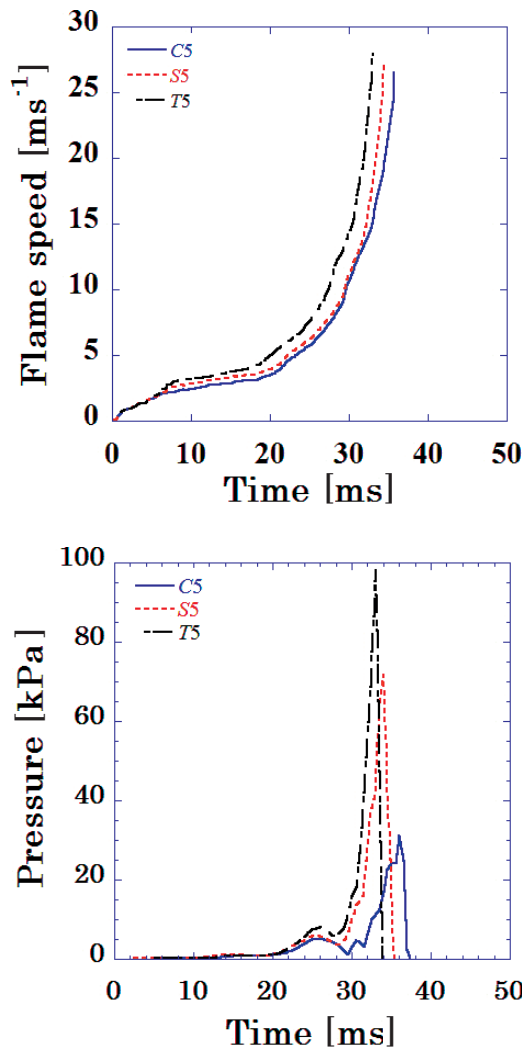


Figure 3 Comparisons of flame speed and overpressure with different shapes for five obstacles.

flame front exited the chamber. As shown in the figure, the fastest flame speed was obtained with the triangular obstacles (T5), 28 ms^{-1} , and the slowest flame speed occurred with the cylindrical obstacle (C5), 26 ms^{-1} . Like the flame speeds, the highest overpressure was obtained with the triangular obstacle (T5), 98 kPa at approximately 33 ms , and the lowest overpressure was obtained with the cylindrical obstacle (C5), 31 kPa at approximately 36 ms . The data for peak overpressures for all the obstacles are shown in Figure 4. The peak overpressures obtained from one or two obstacles were less affected by the obstacle types. However, with multiple obstacles, there were significant differences in observed peak overpressure with the triangular obstacles causing the highest peak overpressure and the cylindrical obstacles causing the lowest. For multiple obstacles, the peak overpressure was highly sensitive to the obstacle geometry.

The main data trend showed that the pressure greatly increased when more than three obstacles were present, regardless of the obstacle type. It was found that the triangular obstructions caused the highest overpressure and the cylindrical obstructions the lowest. This reason may be linked to the presence of surface edges on the obstacle types used. As the propagating flame interacted with the triangular obstacle, with more sharp edges than

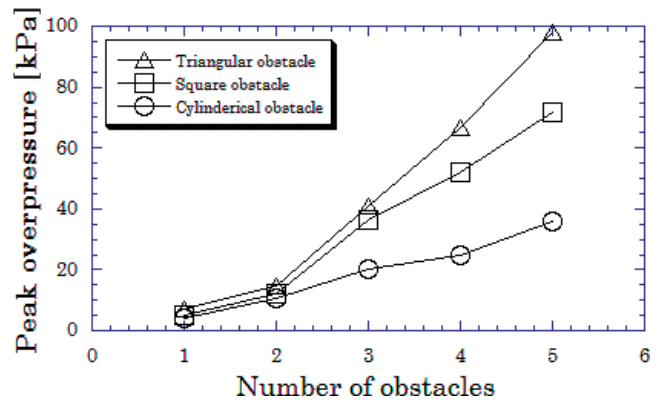


Figure 4 Variations of peak overpressures against the number of different obstacle types.

the others, more large-scale eddies were formed in the wake of the obstacle. The existence of such eddies can significantly increase the turbulence level¹⁸⁾. Flame acceleration and overpressure were mainly dependent on the degree of turbulence. The data given from this study are expected to enable important progress for the validation of numerical models linked to gas explosion predictions. However, further studies are required to quantify the turbulent flow fields behind consecutive obstacles of various shapes positioned ahead of a propagating flame using advanced laser systems.

4. Conclusions

Experimental studies were performed to investigate explosion characteristics by varying the number of obstacles and using three kinds of obstacle shapes: square, triangular, and cylindrical.

As the number of obstacles increased, the flame structures generated in the wake of the obstacles were more chaotic, with a much greater flame surface area. The triangular obstacles caused the fastest flame development, and the cylindrical obstacles the slowest flame development. Like the flame developments, the pressure increased as the number of obstacles increased. The cylindrical obstacles caused the lowest overpressure, and the highest overpressure was caused by the triangular obstacles. The peak overpressure was highly dependent on the obstacle type for multiple obstacles. This result may be linked to the surface edges on the different obstacle types. Large-scale eddies generated behind the triangular obstacle, with more sharp edges in the propagating flame path, caused higher turbulence than the circular obstacle without any edges. The flame propagation speed and deflagration pressure were sensitive to the degree of turbulence. However, further investigations are necessary to quantify the turbulent flow fields in the wake of various obstacle types using advanced three dimensional laser systems and to validate numerical tools related to predictions of deflagration explosions.

References

- 1) N.I. Kim and D.J. Park, Sci. Tech. Energetic Materials, 77, 149–152 (2016).

- 2) G. T. Taylor, Proc. Royal Society, A186, 273 (1946).
- 3) D. Kim, S. Usuba, Y. Watanabe, T. Nario, and Y. Kakudate, Sci. Tech. Energetic Materials, 73, 42–46 (2012).
- 4) D. Kim, Sci. Tech. Energetic Materials, 73, 20–22 (2012).
- 5) J. Yanez, A. Lelyakin, T. Jordan, V. Alekseev, and M. Kuznetsov, Sci. Tech. Energetic Materials, 72, 86–89 (2011).
- 6) D. J. Park and Y. S. Lee, Korean J. Chem. Eng., 26, 313–323 (2009).
- 7) N.R. Popat, C.A. Catlin, B.J. Arntzen, R.P. Lindstedt, B.H. Hjertager, T. Solberg, O. Saeter, and A.C. Van den Berg, J. Hazardous Materials, 45, 1–25 (1996).
- 8) D.J. Park, Y.S. Lee, A.R. Green, and N.Y. Park, 6th Asia-Oceania Symposium on Fire Science and Technology, Daegu, Korea, 161–171 (2004).
- 9) D.K. Pritchard, D.J. Freeman, and P.W. Guilbert, J. Loss. Prev. Process Ind., 9, 205–215 (1996).
- 10) M. Fairweather, G.K. Hargrave, S.S. Ibrahim, and D.G. Walker, Combustion and Flame, 116, 504–518 (1999).
- 11) H. Phylaktou and G.E. Andrews, Combust Sci Tech, 77, 27–39 (1991).
- 12) I.O. Moen, M. Donato, R. Knystautas, and J.H. Lee, Combustion and Flame, 39, 21–32(1980).
- 13) A.R. Masri, S.S. Ibrahim, N. Nehzat, and A.R. Green, Exp Thermal Fluid Sci, 21, 109–116 (2000).
- 14) S.S. Ibrahim, G.K. Hargrave, and T.C. Williams, Exp Thermal Fluid Sci, 24, 99–106 (2001).
- 15) S.S. Ibrahim and A.R. Masri, J Loss Prev Process Ind, 14, 213–221 (2001).
- 16) P. Chen, Y. Li, F. Huang, S. Guo, and X. Liu, J. Loss. Prev. Process Ind., 41, 48–54 (2016).
- 17) D.J. Park, Y.S. Lee, and A.R. Green, J. Hazardous Materials, 153, 340–350 (2008).
- 18) Q. Wang, S. Liu, C. S. Y. Ding, and Z. Li, Energies, 10, 1908–1921 (2017).